Regulation of TRPML1 channel activity and inflammatory exosome release by endogenously produced reactive oxygen species in mouse podocytes

Guangbi Li, Dandan Huang, Ningjun Li, Joseph K. Ritter, Pin-Lan Li [*]

Department of Pharmacology and Toxicology, School of Medicine, Virginia Commonwealth University, Richmond, VA, USA

A B S T R A C T

The nucleotide-binding oligomerization domain-like receptor containing pyrin domain 3 (NLRP3) inflammasome in podocytes has been implicated in the initiation of glomerular inflammation during hyperhomocysteinemia (hHcy). However, the mechanism by which NLRP3 inflammasome products are released from podocytes remains unknown. The present study tested whether exosome secretion from podocytes is enhanced by NADPH oxidase-produced reactive oxygen species (ROS), which may serve as a pathogenic mechanism mediating the release of inflammatory cytokines produced by the NLRP3 inflammasome in podocytes after Hcy stimulation. We first demonstrated the remarkable elevation of endogenously produced ROS in podocytes treated with Hcy compared with control podocytes, which was abolished by pre-treatment with the NADPH oxidase inhibitors, gp91 ds-tat peptide and diphenyleneiodonium (DPI). In addition, Hcy induced activation in podocytes of NLRP3 inflammasomes and the formation of multivesicular bodies (MVBs) containing inflammatory cytokines, which were prevented by treatment with gp91 ds-tat or the ROS scavenger, catalase. Given the importance of the transient receptor potential mucolipin 1 (TRPML1) channel in Ca^{2+}-dependent lysosome trafficking and consequent lysosome-MVB interaction, we tested whether lysosomal Ca^{2+} release through TRPML1 channels is inhibited by endogenously produced ROS in podocytes after Hcy stimulation. By GCaMP3 Ca^{2+} imaging, we confirmed the inhibition of TRPML1 channel activity by Hcy which was remarkably ameliorated by catalase and gp91 ds-tat peptide. By structured illumination microscopy (SIM) and nanoparticle tracking analysis (NTA), we found that ML-SA1, a TRPML1 channel agonist, significantly enhanced lysosome-MVB interaction and reduced exosome release in podocytes, which were attenuated by Hcy. Pre-treatment of podocytes with catalase or gp91 ds-tat peptide restored ML-SA1-induced changes in lysosome-MVB interaction and exosome secretion. Moreover, we found that hydrogen peroxide (H_2O_2) mimicked the effect of Hcy on TRPML1 channel activity, lysosome-MVB interaction, and exosome secretion in podocytes. Based on these results, we conclude that endogenously produced ROS importantly contributes to inflammatory exosome secretion from podocytes through inhibition of TRPML1 channel activity, which may contribute to the initiation of glomerular inflammation during hHcy.

1. Introduction

As a pathogenic mechanism, the nucleotide-binding oligomerization domain-like receptor containing pyrin domain 3 (NLRP3) inflammasome activation in podocytes importantly contributes to hyperhomocysteinemia (hHcy)-induced glomerular injury, glomerular sclerosis, and ultimate end stage renal disease [1–4]. However, it remains unknown how the products of NLRP3 inflammasome activation by podocytes such as IL-1β, IL-18, and high mobility group protein B1 (HMGB1) are released from podocytes to trigger the initial inflammatory events responsible for glomerular injury. The classical Golgi apparatus-mediated delivery pathway may not mediate the secretion of NLRP3 inflammasome products since the activation of NLRP3 inflammasomes occurs in the cytosol. Based on previous studies, it is possible that exosomes mediate the secretion of inflammatory cytokines into the extracellular space [5,6]. As a subtype of extracellular vesicles (EVs), exosomes have been demonstrated to be an important mediator of cell-to-cell communication. Both physiologic and pathophysiologic processes are mediated by their delivery of mRNAs, miRNAs, proteins, and other constituents to acceptor cells [7,8]. As an inflammatory

---

cytokine, IL-1β has also been reported to be a cargo of exosomes [9]. Recently, exosomes have been recognized as a biomarker of glomerular diseases and are implicated as a pathogenic factor in kidney disease [10–15]. These studies support the hypothesis that exosomes may mediate the secretion of NLRP3 inflammasome products out of podocytes, leading to glomerular inflammation and sclerosis. However, the regulatory mechanisms of inflammatory exosome release in podocytes under pathological conditions remain poorly understood.

When multivesicular bodies (MVBs) fuse with the plasma membrane, their contained exosomes are released into the extracellular space. Increasing evidence has shown that lysosomes mediate MVB degradation and thereby control the secretion of exosomes as the content of MVBs [16–21]. In our previous studies, it has been reported that reactive oxygen species (ROS) may act as second messengers to activate NLRP3 inflammasomes in podocytes during hHcy [22]. In addition, hHcy-induced ROS production in podocytes may be attributed to the activation of nicotinamide adenine dinucleotide phosphate (NADPH) oxidase [23]. Given the previous studies indicating that high levels of ROS impair lysosomal function and thereby inhibit autophagic flux in various cell types during hyperglycemia or glucose deprivation [24,25], we considered that NADPH oxidase-dependent ROS production may be involved in lysosomal control of inflammatory exosome release from podocytes during hHcy. Our recent studies have also demonstrated that the lysosomal TRPML1 channel plays an essential role in the regulation of lysosome-MVB interaction and exosome secretion from podocytes [26,27]. Therefore, it would be interesting to test whether lysosomal Ca^{2+} release through TRPML1 channel is involved in the control of inflammatory exosome secretion from podocytes triggered by hHcy.

The present study tested the hypothesis that hHcy-induced ROS production may not only induce the activation of NLRP3 inflammasomes but also promote inflammatory exosome release from podocytes, together triggering local glomerular inflammation and sclerosis. To test this hypothesis, we first examined whether activation of NLRP3 inflammasome and formation of MVBs containing inflammatory cytokines in podocytes are attributed to Hcy-induced endogenous ROS production. Then, we determined the effect of endogenous ROS on lysosomal Ca^{2+} release through the TRPML1 channel in podocytes treated with Hcy. The role of Hcy-induced endogenous ROS production in the regulation of lysosome-MVB interaction and exosome release was also examined. Finally, we tested whether H_2O_2 as a common endogenous ROS can mimic the effect of Hcy on TRPML1 channel activity, lysosome-MVB interaction, and exosome secretion in podocytes. Our findings have demonstrated that endogenous production of ROS importantly contributes to inflammatory exosome secretion from podocytes through inhibition of TRPML1 channel activity, which may contribute to the initiation of glomerular inflammation during hHcy.

2. Materials and methods

2.1. Cell culture

Conditionally immortalized mouse podocytes were cultured and maintained as described previously [26]. Briefly, they were grown at the permissive temperature (33 °C) on collagen I-coated flasks or plates in RPMI 1640 medium supplemented with 10% fetal bovine serum and 10 U/mL recombinant mouse interferon-γ. The podocytes were then passaged and allowed to differentiate at 37 °C for 10–14 days without interferon-γ before use in the experiments described below. Podocytes were treated with ʟ-homocysteine, which is considered to be the pathogenic form of Hcy, at a concentration of 40 μM for 24 h, a dose and treatment time chosen based on previous studies [3,4]. ROS scavenger, catalase (50 U/ml), and pharmacological NADPH oxidase inhibitors, diphenyleneiodonium (10 μM), and gp91ds-tat peptide (5 μM) were added to the cells 1 h before Hcy treatment.

2.2. Electron spin resonance spectrometric analysis of superoxide production

Protein from cultured podocytes was extracted using a sucrose buffer, and then prepared for analysis by resuspension in a modified Krebs–Hepes buffer containing deferoximine (100 μM; MilliporeSigma) and diethyldithiocarbamate (5 μM; MilliporeSigma). To measure NADPH oxidase-dependent superoxide production, 1 mM NADPH substrate was added to 50 μg protein, and each sample was read twice and examined in the presence or absence of superoxide dismutase (SOD; 200 U/ml; MilliporeSigma). 1-Hydroxy-3-methoxycarbonyl-2,2,5,5-tetramethylpyrrolidine (CMH; 1 mM), a superoxide-specific spin-trapping compound, was added to the sample before being loaded into a glass capillary, and analyzed in an electron spin resonance (ESR) spectrometer for 10 min. Results were obtained by taking the difference between the total CMH signal without SOD and the SOD-specific signal, and all values were expressed as the fold changes of the control [23].

2.3. Confocal microscopy

Double-immunofluorescence staining was performed using cultured podocytes grown on collagen-coated glass coverslips [1,28]. Briefly, after treatments followed by fixation, the cells were incubated with goat anti-NLRP3 antibody (1:100; Abcam Biotechnology, Cambridge, United Kingdom), rabbit anti-ASC antibody (1:100; MilliporeSigma, Munich, Germany), rabbit anti-caspase-1 antibody (1:100; Abcam Biotechnology, Cambridge, United Kingdom), rabbit anti-Rab7a antibody (1:100; Abcam Biotechnology, Cambridge, United Kingdom), rabbit anti-VPS16 antibody (1:100; Proteintech, Rosemont, IL, USA), and rat anti-IL-1β antibody (1:100; R&D, Minneapolis, MN, USA) overnight at 4 °C. After slides being washed, Alexa 488-labeled anti-goat secondary antibody (1:200; Life Technologies, CA, USA), Alexa 594-labeled anti-rabbit secondary antibody (1:200; Life Technologies, CA, USA), Alexa 488-labeled anti-rabbit secondary antibody (1:200; Life Technologies, CA, USA), and Alexa 594-labeled anti-rat secondary antibody (1:200; Life Technologies, CA, USA) were added to the cell slides and incubated for 1 h at room temperature. Slides were then washed, stained with DAPI, mounted, and observed using a confocal laser scanning microscope (Fluoview FV1000, Olympus, Japan). Image Pro Plus 6.0 software (Media Cybernetics, Bethesda, MD, USA) was employed to analyze colocalization, expressed as the Pearson correlation coefficient.

2.4. GCaMP3 Ca^{2+} imaging

At 18–24 h after nucleofection with GCaMP3-ML1, podocytes were used for experiments [26]. The fluorescence intensity at 470 nm excitation (F470) was recorded with a Nikon Diaphoto TMD Inverted Fluorescence Microscope. Metafluor imaging and analysis software were used to acquire, digitize and store the images for offline processing and statistical analysis (Universal Imaging, Bedford Hills, NY, USA). Lysosomal Ca^{2+} release was measured under a 'low' external Ca^{2+} solution, which contained 145 mM NaCl, 5 mM KCl, 3 mM $MgCl_2$, 10 mM glucose, 1 mM EGTA and 20 mM HEPES (pH 7.4). The response to ML-SA1 (20 μM), a TRPML channel agonist and activator of lysosomal Ca^{2+} release, was determined. The Ca^{2+} ionophore, ionomycin (1 μM) was used as a positive control in the podocytes. After GCaMP3 Ca^{2+} imaging, we compared the peak value of $\Delta F/F_0$ ((intracellular F470 intensity at n second−intracellular F470 intensity at 0 s)/intracellular F470 intensity at 0 s) between additions of ML-SA1 and ionomycin to solution.

2.5. Nanoparticle tracking analysis

Nanoparticle tracking analysis (NTA) measurements were performed with a NanoSight NTA3.2 Dev Build 3.2.16 (Malvern Instruments Ltd., UK), equipped with a sample chamber with a 638-nm laser and a Viton fluoroelastomer O-ring. The samples were injected into the sample

chamber with sterile syringes (BD, New Jersey, USA) until the liquid reached the tip of the nozzle. All measurements were performed at room temperature. The screen gain and camera level settings were 10 and 13, respectively. Each sample was measured at standard measurement, 30 s with manual shutter and gain adjustments. Each sample was analyzed in triplicate. 3D figures were exported from the software. Particles sized between 50 and 100 nm were calculated [26].

2.6. Structured illumination microscopy

After treatments followed by fixation, the cells were incubated with rabbit anti-Rab7a antibody (1:100; Abcam Biotechnology, Cambridge, United Kingdom) and rat anti-Lamp-1 antibody (1:100; Abcam Biotechnology, Cambridge, United Kingdom) overnight at 4 °C. After slides being washed, Alexa 488-labeled anti-rabbit secondary antibody (1:200; Life Technologies, CA, USA) and Alexa 594-labeled anti-rat secondary antibody (1:200; Life Technologies, CA, USA) were added to the cell slides and incubated for 1 h at room temperature. Slides were then washed, stained with DAPI, and mounted. A Nikon fluorescence microscope in the structured illumination microscopy (SIM) mode was used to obtain images. Image Pro Plus 6.0 software (Media Cybernetics, Bethesda, MD, USA) was employed to analyze colocalization, expressed as the Pearson correlation coefficient.

2.7. Statistical analysis

Data are expressed as mean ± SEM, where significance was determined using one-way ANOVA followed by the Student-Newman-Keuls post hoc test. χ^2 test was used to determine significance of ratio and percentage data. $P < 0.05$ was considered statistically significant.

3. Results

3.1. Formation of MVBs containing inflammatory cytokines in podocytes after Hcy stimulation

To determine whether NADPH oxidase-derived superoxide contributes to NLRP3 inflammasome activation by Hcy, we first examined the effect of Hcy on the relative superoxide level in podocytes in the presence and absence of NADPH oxidase inhibitors. By ESR analysis, Hcy treatment at a concentration of 40 μM for 24 h was found to induce superoxide production, and this effect was blocked by inclusion of an NADPH oxidase inhibitors, either gp91ds-tat peptide (5 μM) or diphenyleneiodonium (10 μM) (Fig. 1). Using confocal microscopy, we demonstrated that Hcy induced formation of NLRP3 inflammasomes as indicated by increased colocalization of inflammasome markers, NLRP3 with ASC, and NLRP3 with caspase-1, in podocytes (Fig. 2A). Pretreatment with the ROS scavenger, catalase (50 U/ml), or gp91 ds-tat peptide, however, blocked this increase. Interestingly, it was found that Hcy also enhanced colocalization of two different MVB markers and the inflammatory cytokine, IL-1β (Rab7a with IL-1β and VPS16 with IL-1β) (Fig. 2B). These data indicate that the level of MVBs containing inflammatory cytokines is increased by Hcy treatment of podocytes. This Hcy-induced increase in was also prevented by co-treatment with catalase or gp91 ds-tat peptide.

3.2. Hcy-induced elevation of exosome release from podocytes

NTA was used to measure exosome release into the medium from Ctrl or Hcy-treated podocytes, in the presence or absence of catalase or gp91 ds-tat peptide. As shown in Fig. 3A, the representative 3-D histograms of exosomes showed that the exosome concentration remained relatively low in culture medium of podocytes under control condition. Exosome concentration was increased by Hcy treatment compared to control podocyte cultures. On the contrary, ML-SA1 remarkably decreased exosome concentration in culture medium of podocytes. Summarized
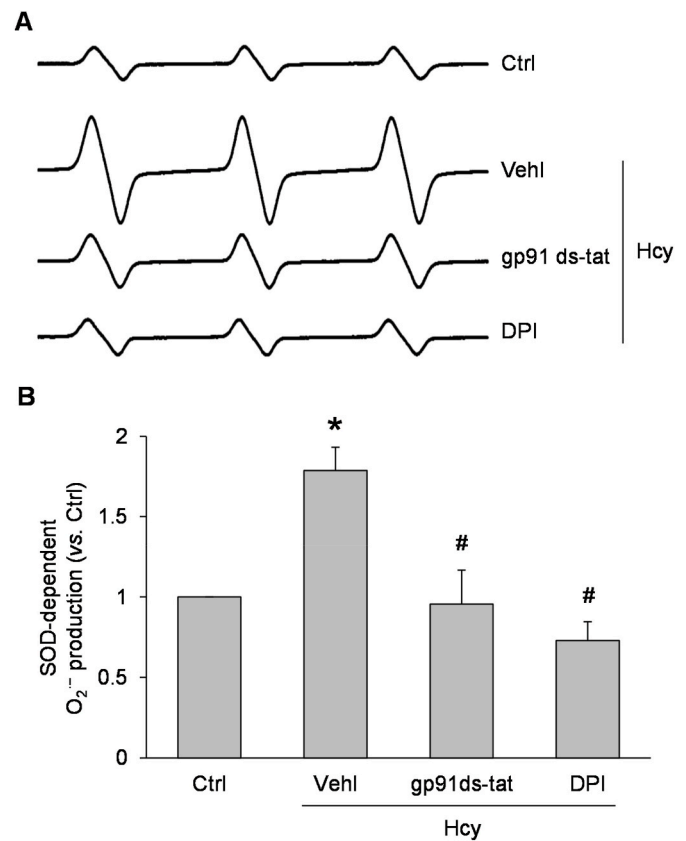

Fig. 1. Formation of reactive oxygen species induced by Hcy treatment of podocytes and blockade by NADPH oxidase inhibitors. A. Representative ESR spectra showing $O_2^{\bullet-}$ production in different groups of podocytes. B. Summarized data showing $O_2^{\bullet-}$ production in different groups of podocytes (n = 6). *p < 0.05 vs. Ctrl group, #p < 0.05 vs. Vehl-Hcy group. Ctrl, control; Vehl, vehicle; gp91 ds-tat, gp91 ds-tat peptide; DPI, diphenyleneiodonium; Hcy, homocysteine.

data demonstrated that Hcy induced a remarkable elevation whereas ML-SA1 significantly reduced exosome secretion from podocytes. Furthermore, pretreatment of podocytes with catalase or gp91 ds-tat peptide markedly attenuated the Hcy-induced increase in exosome secretion from podocytes (Fig. 3B).

3.3. Inhibition of lysosomal Ca^{2+} release through TRPML1 channel by Hcy

Given that lysosomal TRPML1 channel-mediated Ca^{2+} release has been reported to be essential for lysosome trafficking and fusion to MVB [26,27], we tested whether lysosomal TRPML1 channel activity can be altered by endogenous ROS after Hcy stimulation. To specifically detect Ca^{2+} release through the lysosomal TRPML1 channel, we used podocytes expressing GCaMP3-ML1, a fusion protein containing the Ca^{2+}-sensing fluorophore, GCaMP3, on the cytoplasmic amino terminus of TRPML1 as described in our previous studies [26]. The fluorescence emitted by GCaMP3 (F470) in podocytes was monitored dynamically and continuously using a fluorescent microscopic imaging system. The intensity of Ca^{2+}-induced GCaMP3 fluorescence indicated the amount of Ca^{2+} released through lysosomal TRPML1 channels. ML-SA1, a TRPML1 channel agonist, induced a rapid elevation of GCaMP3 fluorescence in podocytes, which was followed by a larger signal increase caused by later addition of ionomycin, a Ca^{2+} ionophore. After Hcy stimulation, ML-SA1 induced a smaller elevation in GCaMP3 fluorescence in podocytes, while ionomycin still stimulated a dramatic elevation of GCaMP3 fluorescence in these cells (Fig. 4C). In addition, pre-treatment of
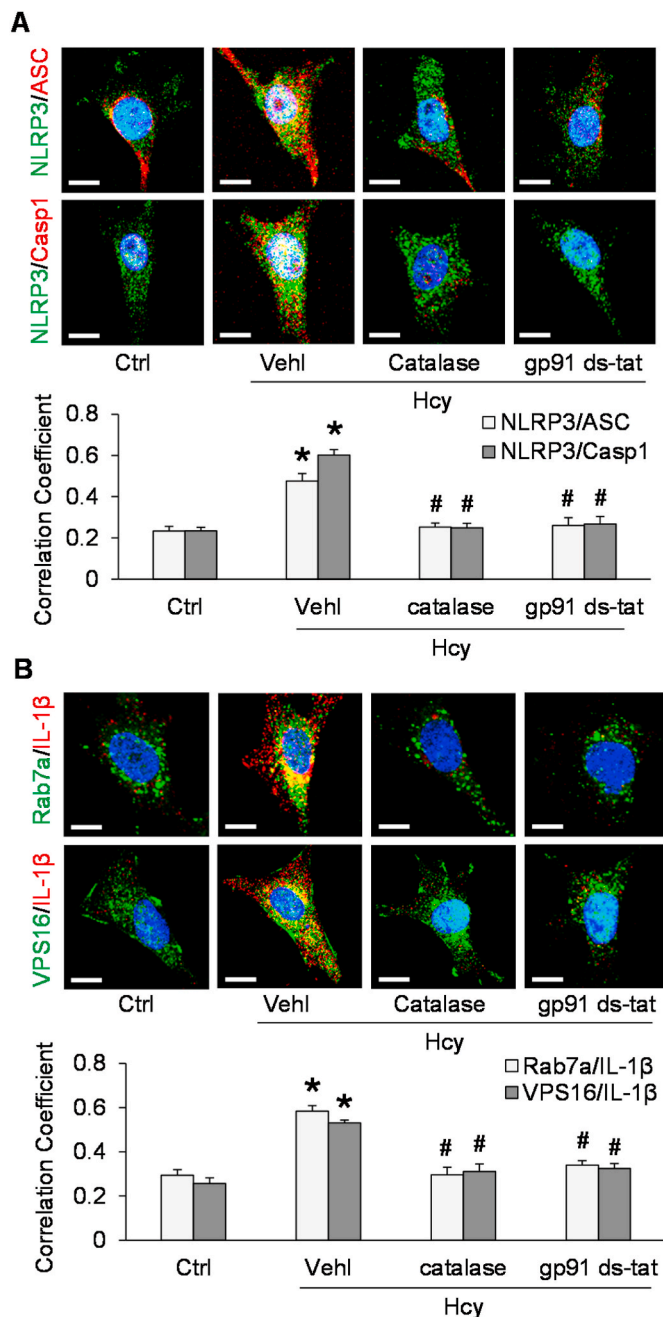
Fig. 2. NLRP3 inflammasome activation and MVB-inflammatory cytokine association after Hcy treatment of podocytes. A. Representative images and summarized data showing the colocalization of inflammasome markers in different groups of podocytes (n = 3–5). Scale bars = 20 μm. B. Representative images and summarized data showing the colocalization of MVB markers and IL-1β in different groups of podocytes (n = 4–5). Scale bars = 20 μm *p < 0.05 vs. Ctrl group, #p < 0.05 vs. Vehl-Hcy group. Ctrl, control; Vehl, vehicle; gp91 ds-tat, gp91 ds-tat peptide; Hcy, homocysteine.

podocytes with catalase or gp91 ds-tat recovered the elevation of GCaMP3 fluorescence induced by ML-SA1.

3.4. Lysosome-MVB interaction attenuated by Hcy

To determine the role of lysosomes in the regulation of exosome release, SIM was performed to detect lysosome-MVB interaction in podocytes after co-transfection with Rab7a-GFP plasmid and Lamp-1-RFP plasmid. Under the control condition, we observed considerable

colocalization of Rab7a (MVB marker, green fluorescence) and Lamp-1 (lysosome marker, red fluorescence), as demonstrated by yellow spots in the overlapping fluorescence image (Fig. 5A). After Hcy stimulation, colocalization of Rab7a and Lamp-1 was significantly reduced compared to control (Fig. 5B). In contrast, activation of TRPML1 channels by ML-SA1 treatment significantly increased the colocalization of Rab7a and Lamp-1 in podocytes, and this effect was attenuated by Hcy. Pretreatment of podocytes with catalase or gp91 ds-tat peptide inhibited the Hcy-induced decrease in lysosome-MVB interaction in podocytes.

3.5. Formation of MVBs containing inflammatory cytokines in podocytes after H_2O_2 stimulation

Recently, we have demonstrated that endogenously produced superoxide and hydrogen peroxide (H_2O_2) primarily contribute to NLRP3 inflammasome formation and activation in mouse glomeruli resulting in glomerular injury during hHcy [22]. To further confirm whether the above pathological changes could be attributed to endogenously produced ROS, we tested whether H_2O_2 can mimic the effects of Hcy in podocytes. By confocal microscopy, NLRP3 inflammasome formation and formation of MVBs containing inflammatory cytokines were detected in these cells before and after treatment with H_2O_2 in different doses for 4 h. As shown in Fig. 6A, H_2O_2 induced formation of NLRP3 inflammasome indicated by colocalization of inflammasome markers (NLRP3 with ASC and NLRP3 with caspase-1) in podocytes in a dose-dependent manner. Correspondingly, we found that colocalization of MVB and inflammatory cytokine markers, Rab7a with IL-1β, and VPS16 with IL-1β) were also elevated by H_2O_2, which was dose-dependent. These findings support that H_2O_2 treatment induces the formation of MVBs containing inflammatory cytokines in podocytes (Fig. 6B).

3.6. Enhancement of exosome secretion from podocytes by H_2O_2

We also tested whether treatment with exogenous H_2O_2 could enhance the release of exosomes from podocytes. As shown in Fig. 7A, the representative 3-D histograms of exosomes showed that the exosome concentration was increased in culture medium of podocytes after H_2O_2 (50 μM) stimulation for 24 h compared with control cells. Summarized data indicated significant increase in exosome release induced by H_2O_2 (Fig. 7B). In contrast, ML-SA1 decreased exosome concentration in culture medium of podocyte, and pretreatment with H_2O_2 blocked this effect of ML-SA1.

3.7. Inhibition of TRPML1 channel activity and lysosome-MVB interaction by H_2O_2

Next, we tested whether H_2O_2 can alter TRPML1 channel-mediated Ca^{2+} release in podocytes. As shown in Fig. 8, ML-SA1 induced a remarkable elevation of GCaMP3 fluorescence in GCaMP3-ML1-transfected podocytes compared to vehicle-treated control. However, the ML-SA1-induced increase in GCaMP3 fluorescence was totally blocked by pretreating the podocytes with H_2O_2. We further analyzed for the effect of H_2O_2 on the lysosome-MVB interaction with or without ML-SA1 treatment using SIM. Under control conditions, a basal level of colocalization of Rab7a (green fluorescence) and Lamp-1 (red fluorescence) was detectable in podocytes, which was further increased by activation of TRPML1 channels with ML-SA1. H_2O_2 treatment reduced the colocalization of Rab7a and Lamp-1 in vehicle-treated control and prevented the inducing effect of ML-SA1 (Fig. 9).

4. Discussion

The major goal of the present study was to determine whether exosome secretion from podocytes is enhanced by NADPH oxidase-produced reactive oxygen species (ROS), which may serve as a
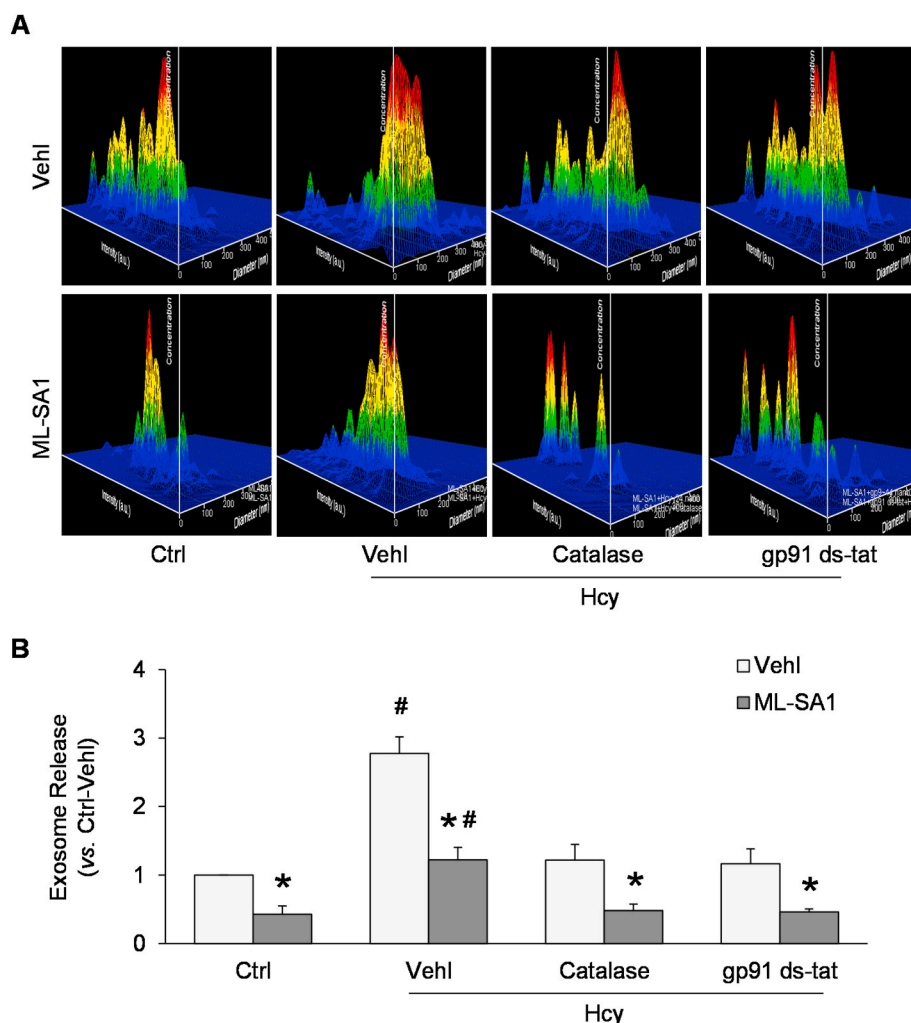
A

B

Fig. 3. Enhanced exosome release from podocytes after Hcy and dependence on ROS and NADPH oxidase. A. Representative images showing exosome release from different groups of podocytes. The x axis is diameter (nm); the y axis is concentration; the z axis is intensity (a.u.). B. Summarized data showing exosome release from different groups of podocytes (n = 6). *p < 0.05 vs. Vehl group, #p < 0.05 vs. Ctrl group. Ctrl, control; Vehl, vehicle; gp91 ds-tat, gp91 ds-tat peptide; Hcy, homocysteine.

pathogenic mechanism mediating the release of inflammatory cytokines produced by the NLRP3 inflammasome in podocytes after Hcy stimulation. Our results demonstrated that Hcy induced activation of the NLRP3 inflammasome and formation of MVBs containing inflammatory cytokines in podocytes, and that these effects were associated with elevated exosome release from the cells. In addition, lysosomal Ca^{2+} release through TRPML1 channel in podocytes was inhibited by Hcy, leading to attenuation of lysosome-MVB interaction. All these pathological changes induced by Hcy were attributed to increased production of endogenous ROS by NADPH oxidase. Moreover, H_2O_2 as a common endogenous ROS mimicked the effect of Hcy on TRPML1 channel activity, lysosome-MVB interaction, and exosome secretion in podocytes (Fig. 10). Our findings indicate that endogenously produced ROS importantly contributes to inflammatory exosome secretion from podocytes through inhibition of TRPML1 channel activity, which may contribute to the initiation of glomerular inflammation during hHcy.

In previous studies, it has been demonstrated that NLRP3 inflammasome activation in podocytes contributes to glomerular inflammation and sclerosis during hHcy [1–4]. NLRP3 inflammasome is composed of three major proteins, including a NOD-like receptor NLRP3, an adaptor protein apoptosis-associated speck-like protein containing a caspase recruitment domain (ASC), and caspase-1 [29]. Both endogenous and exogenous danger signals can be recognized by NLRP3, leading to recruitment and aggregation of ASC and caspase-1 to form a protein complex, where caspase-1 is activated [30–32]. Pro-IL-1β and pro-IL-18 are proteolytically cleaved by active caspase-1, leading to the production of biologically active IL-1β and IL-18. Moreover, active caspase-1

may produce other danger molecules like damage-associated molecular patterns. However, these products of NLRP3 inflammasome may not be secreted out of podocytes via a classical and Golgi apparatus-mediated delivery pathway given that the activation of NLRP3 inflammasome mainly occurs in the cytosol. It remains unknown how NLRP3 inflammasome products such as inflammatory cytokines are released out of podocytes and thereby induce glomerular inflammation during hHcy. Recently, it has been found that exosomes importantly contribute to the release of signaling molecules to the extracellular space [33]. It is possible that the secretion of inflammatory cytokines from podocytes is mediated by exosomes. Given the important role of endogenously produced ROS in NLRP3 inflammasome activation and podocyte injury induced by hHcy [23] and in the regulation of lysosomal function [24,25], the present study tested whether endogenous ROS production by NADPH oxidase contributes to NLRP3 inflammasome activation and inflammatory exosome release in podocytes after Hcy stimulation.

By various approaches, activation of NLRP3 inflammasome, formation of MVBs containing NLRP3 inflammasome products, and elevated exosome release were observed in podocytes after Hcy stimulation. However, in podocytes pre-treated with catalase or gp91 ds-tat, these pathological changes were blocked. These results clearly suggest that NADPH oxidase-dependent ROS production contributes to Hcy-induced NLRP3 inflammasome activation in podocytes. In addition, exosomes may mediate the secretion of inflammatory cytokines from podocytes. Under physiological condition, intercellular communication is mediated by exosomes in kidney; under pathological condition, the development
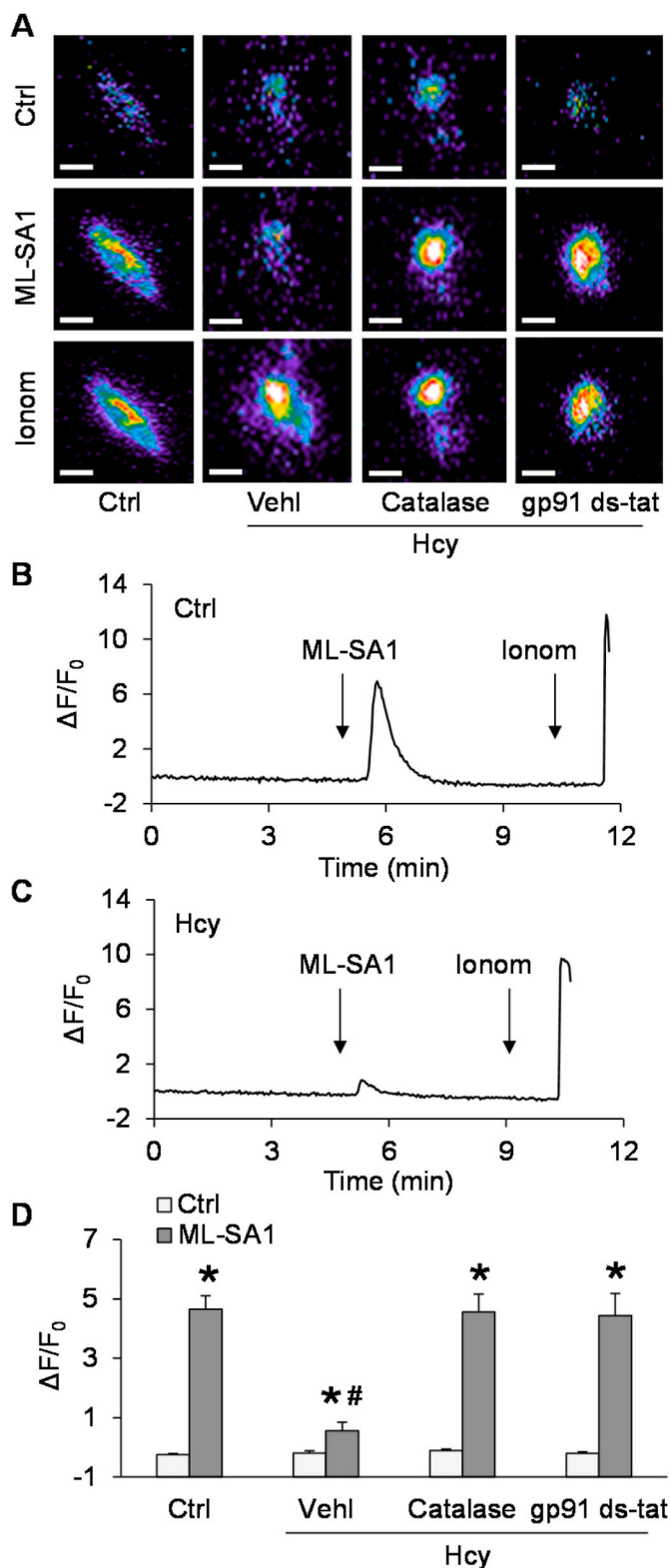
A

B

C

D

Fig. 4. Inhibition of lysosomal Ca^{2+} release through TRPML1 channel by Hcy. A. Representative images showing GCaMP3 fluorescence in different groups of podocytes. Scale bars = 40 μm. B. A representative curve showing that ML-SA1 induced remarkable elevation of GCaMP3 signal in podocytes under control condition. C. A representative curve showing that ML-SA1 induced small elevation of GCaMP3 signal in podocytes after Hcy stimulation. D. Summarized data showing GCaMP3 fluorescence in different groups of podocytes (n = 5–9). *p < 0.05 vs. Vehl group, #p < 0.05 vs. Ctrl group. Ctrl, control; Vehl, vehicle; gp91 ds-tat, gp91 ds-tat peptide; Hcy, homocysteine.
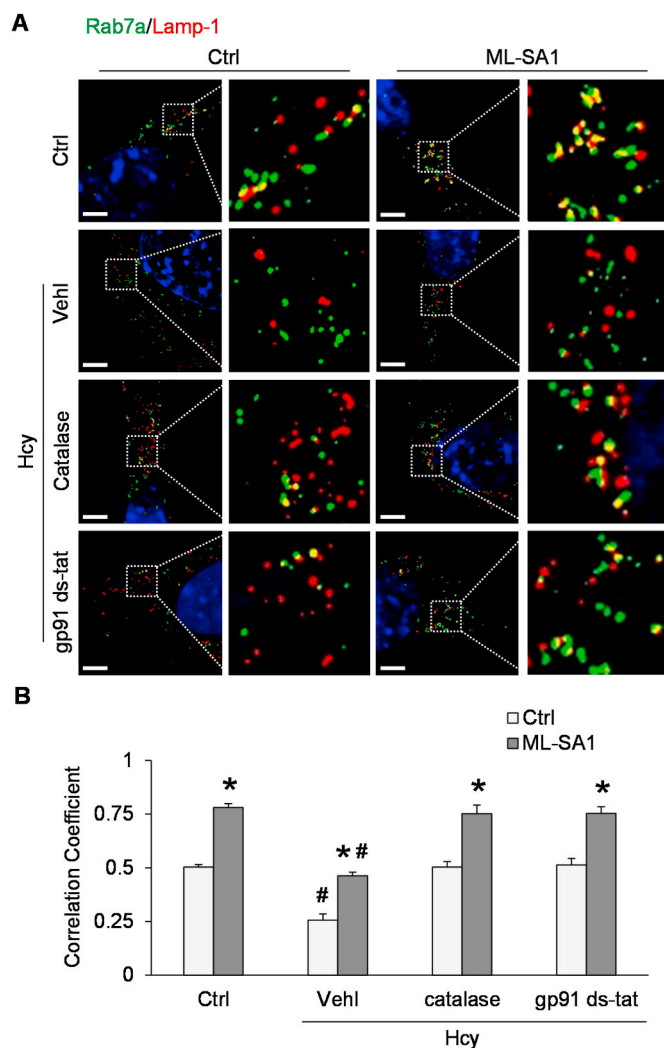
A Rab7a/Lamp-1

B

Fig. 5. Attenuation of lysosome-MVB interaction by Hcy treatment of podocytes. A. Representative images showing the colocalization of Rab7a-GFP and Lamp-1-RFP in different groups of podocytes. Scale bars = 5 μm. B. Summarized data showing the colocalization of Rab7a-GFP and Lamp-1-RFP in different groups of podocytes (n = 6–8). *p < 0.05 vs. Vehl group, #p < 0.05 vs. Ctrl group. Ctrl, control; Vehl, vehicle; gp91 ds-tat, gp91 ds-tat peptide; Hcy, homocysteine.

of renal disease is attributed to exosomes [16]. It has been reported that diabetic mice had increased exosomes containing podocalyxin, a glycoconjugate on the podocyte apical surface, in their urine even before the onset of albuminuria [34]. Increased exosomes may serve as a signaling vesicle to trigger phenotypic changes in neighboring cells [35] and they also participate in the development of albuminuria [36]. Clinically, it has been found that elevated release of exosomes from podocytes is associated with albuminuria and glomerular degeneration in some patients with focal segmental glomerulosclerosis (FSGS) and nephrotic syndrome (NS) [16–21]. Recently, it has been reported that exosomes mediate the release of NLRP3 inflammasome products to the extracellular space in response to D-ribose stimulation [37]. However, the molecular mechanism mediating the secretion of inflammatory cytokines during hHcy remains unknown. To our knowledge, the results from the present study provide the first experimental evidence that the release of NLRP3 inflammasome products from podocytes may be attributed to exosomes, which may be an important pathogenic mechanism responsible for glomerular inflammation during hHcy. Moreover, NADPH oxidase-dependent ROS production not only switches on NLRP3 inflammasome assembly but also regulates inflammatory exosome
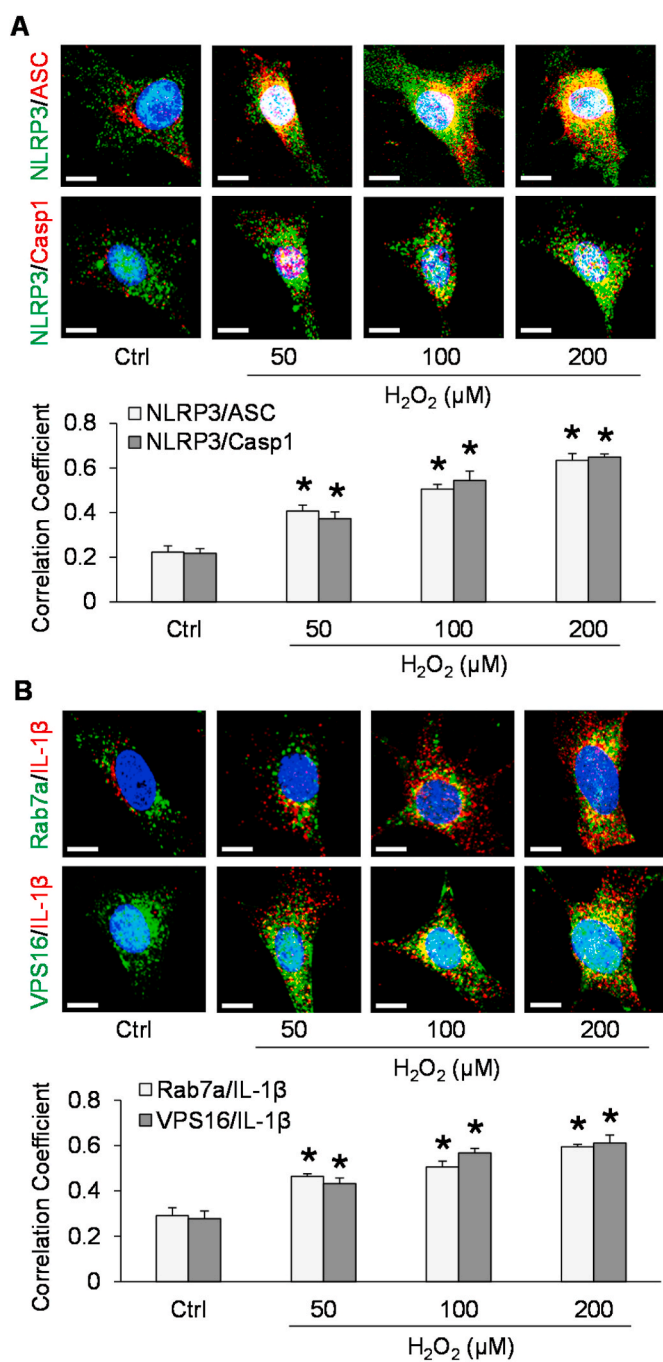
Fig. 6. Formation of NLRP3 inflammasomes and MVBs containing inflammatory cytokines in podocytes after H_2O_2 stimulation. A. Representative images and summarized data showing the colocalization of inflammasome markers in different groups of podocytes (n = 3–5). Scale bars = 20 μm. B. Representative images and summarized data showing the colocalization of MVB markers and IL-1β in different groups of podocytes (n = 4–5). Scale bars = 20 μm *p < 0.05 vs. Ctrl group. Ctrl, control; H_2O_2, hydrogen peroxide.

Fig. 7. Enhancement of exosome secretion from podocytes by H_2O_2. A. Representative images showing exosome release from different groups of podocytes. The x axis is diameter (nm); the y axis is concentration; the z axis is intensity (a.u.). B. Summarized data showing exosome release from different groups of podocytes (n = 6). *p < 0.05 vs. Vehl group, #p < 0.05 vs. Ctrl group. Ctrl, control; Vehl, vehicle; H_2O_2, hydrogen peroxide.

release in podocytes after Hcy stimulation.

Another interesting finding of the present study is that Hcy inhibited TRPML1 channel activity and lysosome-MVB interaction in podocytes. Nevertheless, these pathological changes were blocked by pre-treatment with catalase or gp91 ds-tat. These results imply that Hcy may reduce lysosome-MVB interaction and lysosome-dependent MVB degradation via inhibition of TRPML1 channel activity, leading to enhancement of inflammatory exosome release. Moreover, ROS produced by NADPH oxidase may be involved in the regulation of TRPML1 channel and
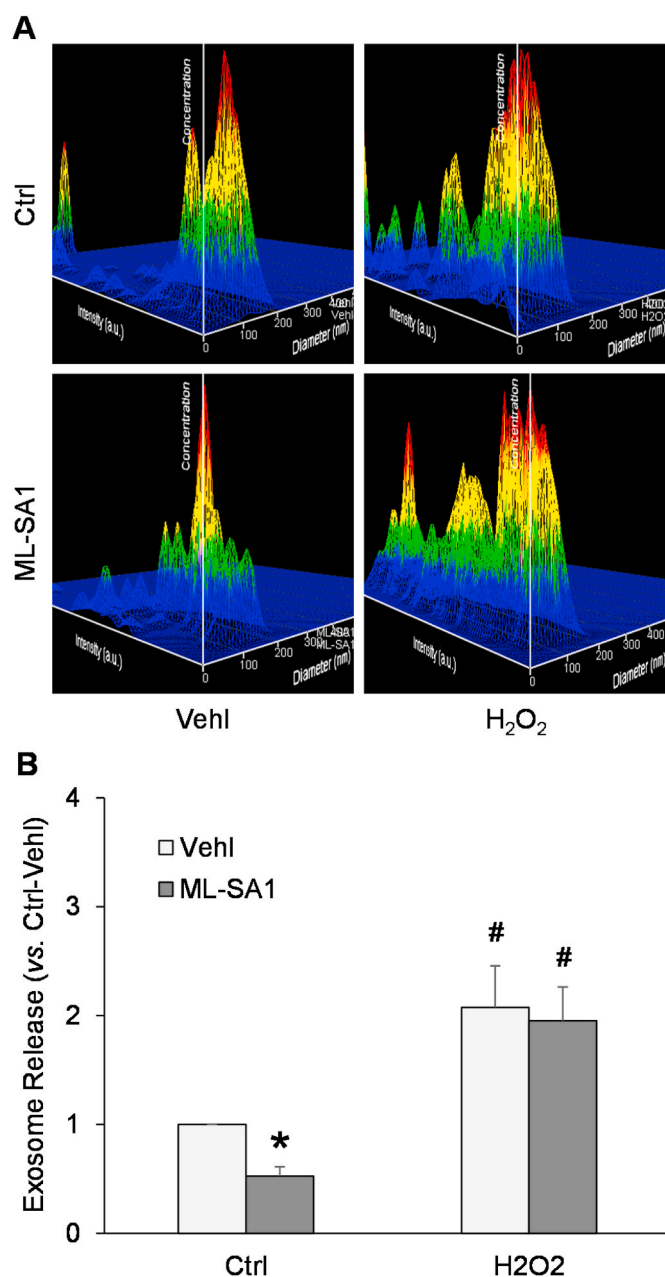
lysosome-MVB interaction by Hcy. Previous studies have shown that lysosomes can actively respond to environmental changes such as increased autophagosomes, MVBs, and other stress signals in podocytes and other cells. Such property of lysosomal function determines the degradation of various intracellular vesicles such as phagosomes, autophagosomes, and MVBs [38–41]. There is evidence that the fusion of lysosomes and MVBs is controlled by the regular trafficking of lysosomes. Such active movement of lysosomes is determined by the lysosomal Ca^{2+} release [40,42]. As an ubiquitously expressed protein, the transient receptor potential-mucolipin-1 (TRPML1) channel is a Ca^{2+} ion channel expressed in intracellular endosomes and lysosomes [43]. The Ca^{2+} enters the lysosomal compartment by H^+/Ca^{2+} exchange and exits through TRPML1 channels in response to endogenously produced
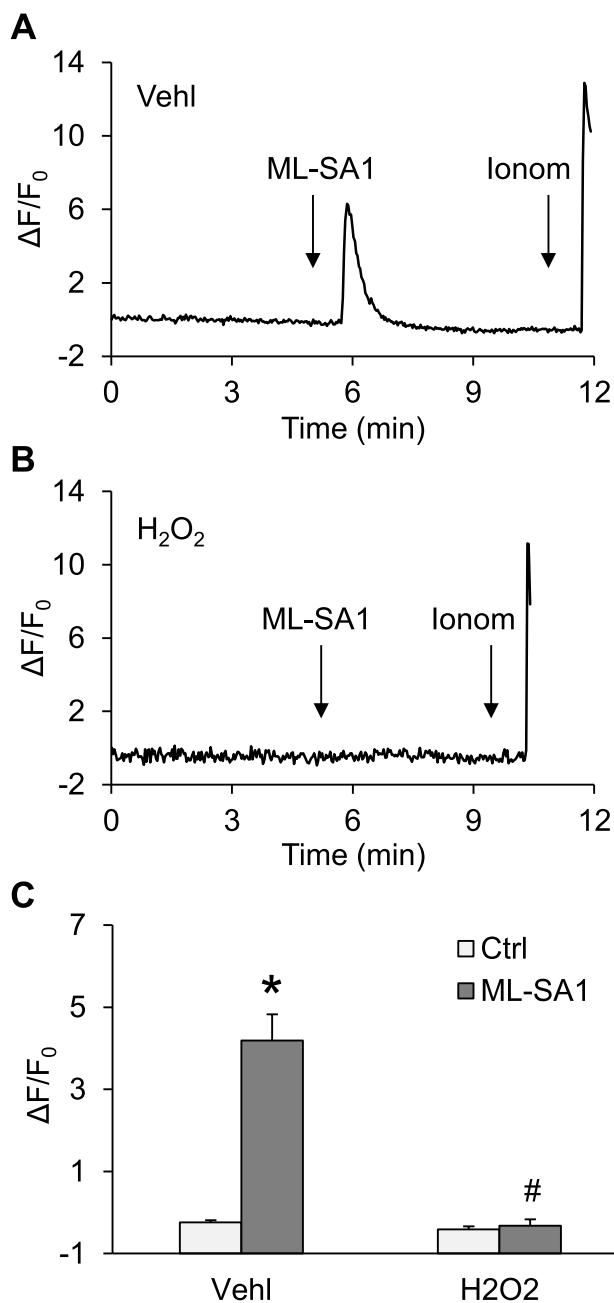
Fig. 8. Blockade of lysosomal TRPML1 channel-mediated Ca^{2+} release in podocytes by H_2O_2. A. A representative curve showing that ML-SA1 induced remarkable elevation of GCaMP3 signal in podocytes pre-treated with vehicle. B. A representative curve showing that ML-SA1 had no effects on GCaMP3 signal in podocytes pre-treated with H_2O_2. C. Summarized data showing GCaMP3 fluorescence in different groups of podocytes (n = 6–8). *p < 0.05 vs. Ctrl group, #p < 0.05 vs. Vehl group. Ctrl group. Ctrl, control; Vehl, vehicle; H_2O_2, hydrogen peroxide.

Fig. 9. Lysosome-MVB interaction in podocytes attenuated by H_2O_2. A. Representative images showing the colocalization of Rab7a-GFP and Lamp-1-RFP in different groups of podocytes. Scale bars = 5 μm. B. Summarized data showing the colocalization of Rab7a-GFP and Lamp-1-RFP in different groups of podocytes (n = 6). *p < 0.05 vs. Vehl group, #p < 0.05 vs. Ctrl group. Ctrl group. Ctrl, control; Vehl, vehicle; H_2O_2, hydrogen peroxide.

NAADP [44–47] or other factors like PIPs (PI(3,5)P2) and ions [48–50]. Recently, we have demonstrated that lysosome trafficking and lysosome-MVB interaction is controlled by TRPML1 channel-mediated Ca^{2+} release in podocytes [26,27]. In podocytes lack of Asah1 gene, the blockade of TRPML1 channel is associated with impaired lysosome-MVB interaction, leading to increased exosome secretion. Consistent with these previous studies, our findings have demonstrated that Hcy-induced robust release of inflammatory exosomes is attributed to altered lysosomal TRPML1 channel activity and lysosome-MVB
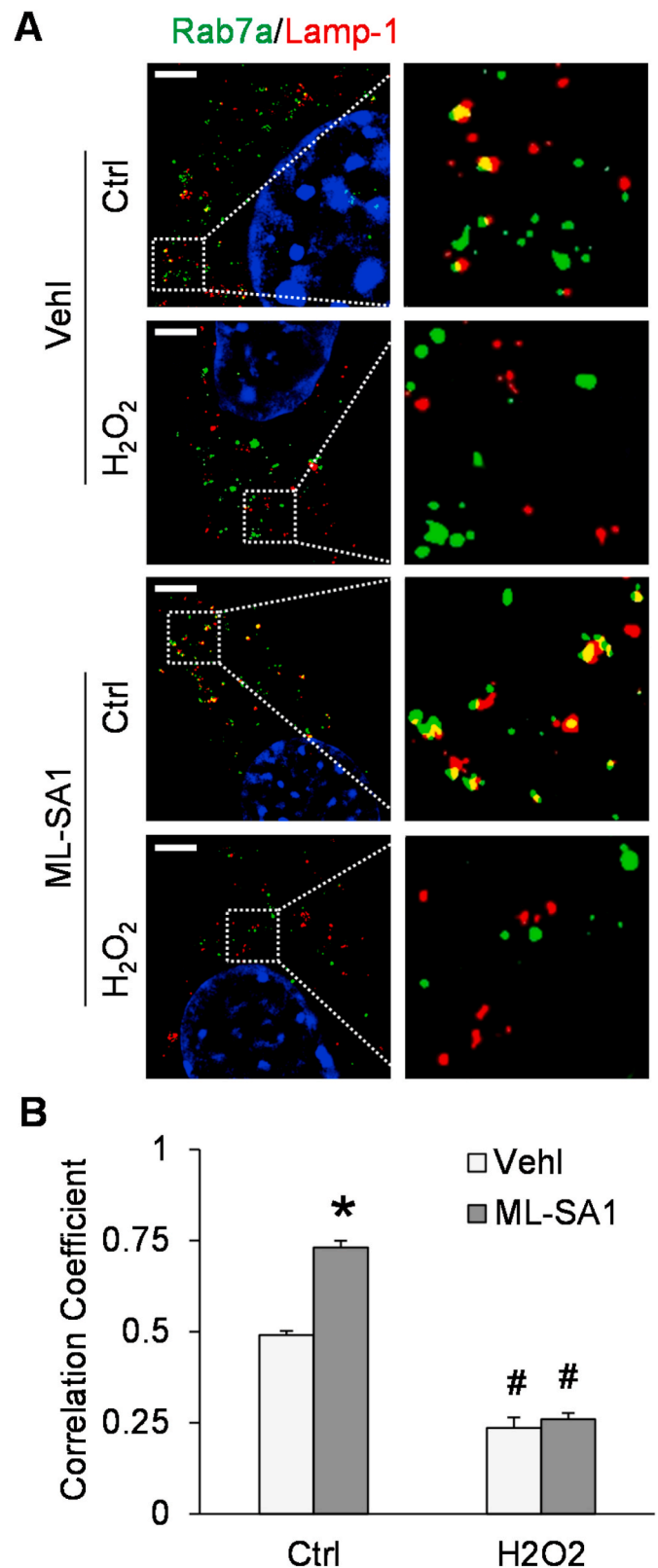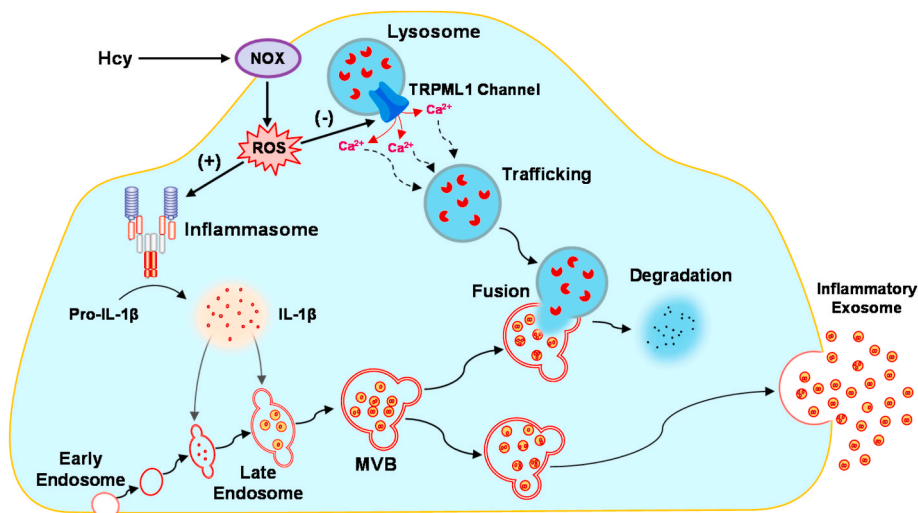
Fig. 10. Regulation of TRPML1 channel activity and inflammatory exosome release by endogenously produced ROS in mouse podocytes. In response to Hcy, NADPH oxidase is activated to produce ROS in podocytes. NLRP3 inflammasomes are activated by ROS to produce inflammatory cytokines such as IL-1β, which enter the late endosomes that form MVBs. At the same time, lysosomal Ca^{2+} release through TRPML1 channel is inhibited by ROS, leading to the impairment of lysosome trafficking and reduction of lysosome-MVB interaction, a process determining the MVB fate. Under such conditions, decreased lysosome degradation of MVBs leads to robust release of MVB contents as inflammatory exosomes from podocytes. Hcy, homocysteine; NOX, NADPH oxidase; ROS, reactive oxygen species; MVB; multivesicular body.

interaction. In addition, our results for the first time link NADPH oxidase-dependent ROS production to the regulation of lysosomal TRPML1 channel activity and lysosome-MVB interaction in podocytes.

To further confirm our findings, we tested whether H$_2$O$_2$ as a common endogenous ROS can mimic the effect of Hcy on TRPML1 channel activity, lysosome-MVB interaction, and exosome secretion in podocytes. Our results showed that H$_2$O$_2$ enhanced activation of NLRP3 inflammasomes, formation of MVBs containing inflammatory cytokines, and release of inflammatory exosomes in a dose-dependent manner. Moreover, H$_2$O$_2$ was found to inhibit TRPML1 channel activity and lysosome-MVB interaction in podocytes. A recent study has focused on the regulation of TRPML1 channel by ROS or oxidants in some cell lines [51]. The actions of a variety of commonly used oxidants on TRPML1 channel have been tested in this study. As a non-selective strong oxidant, chloramine-T was found to induce the opening of TRPML1 channel with a potency comparable to those of PI(3,5)P2 and ML-SA1. Meanwhile, it was found that several other commonly used oxidants, including NaOCl, N-chlorosuccinimide, H$_2$O$_2$, t-butyl hydroperoxide (TBHP), and thimerosal, activated the TRPML1 channel less potently. However, cysteine-modifying oxidants such as DTNB and DTNP did not affect the activity of TRPML1 channel. Similarly, 4-HNE, a reactive lipid peroxidation intermediate, and SNAP, a NO-donor, failed to induce the opening of TRPML1 channel. Among these different oxidants, only H$_2$O$_2$ mimicked the mitochondrial ROS, although the dose of H$_2$O$_2$ used in the study was extremely high (10 mM). These results suggest that different forms of ROS or oxidants at different levels may play diverse roles in the regulation of TRPML1 channel activity. Functionally, carbonyl cyanide m-chlorophenylhydrazone (CCCP), a mitochondrial respiration inhibitor commonly used to induce ROS production, was found to induce autophagic clearance of damaged mitochondria through activation of TRPML1 channel [51]. Conversely, another previous study has shown that CCCP induced autophagosome accumulation and apoptosis through activation of TRPML1 channels [52]. It has been found that many compounds, including N-acetylcysteine, ferulic acid, and trehalose, reduce ROS and enhance autophagy simultaneously [53–55]. These findings may support the possibility that ROS inhibits lysosome function through blockade of TRPML1 channels. In the present study, our findings suggest that ROS may contribute to inflammatory exosome release from podocytes by inhibition of TRPML1 channel activity under pathological conditions, such as hHcy.

In addition to podocyte, the pathological role of ROS has been reported in other cell types such as endothelial cells and smooth muscle cells [56,57]. During obesity, visfatin-induced NLRP3 inflammasome activation in vascular endothelial cells importantly contributes to the initiation of endothelial inflammatory response, leading to arterial inflammation and endothelial dysfunction in mice [58]. This action of visfatin is attributed to ROS production by NADPH oxidase [59]. In mice fed with high-fat diet, NADPH oxidase-dependent ROS production in smooth muscle cells contributes to exercise intolerance, vascular inflammation, and augmented adipogenesis in mice fed with high-fat diet [60]. Smooth muscle-specific knockout of p22^{phox}, a NADPH oxidase subunit, has been found to block high-fat diet-induced weight gain and leptin resistance and reduce T-cell infiltration to perivascular fat [60]. Recently, it has been reported that NADPH oxidase-dependent ROS production induces lung endothelial cell dysfunction via activation of CaMKII/ERK1/2/MLCK pathway [61]. These findings imply that in addition to inflammatory pathways endogenously produced ROS may contribute to the pathogenesis via noninflammatory pathways. In our future study, it would be interesting to test whether NADPH oxidase-dependent ROS production induces podocyte injury during hHcy via noninflammatory pathways.

In summary, the present study demonstrated that Hcy inhibited lysosomal TRPML1 channel activity via enhancement of ROS production by NADPH oxidase, which caused less lysosome-MVB interaction and more exosome release in podocytes. These exosomes may mediate the secretion of NLRP3 inflammasome products in podocytes after Hcy stimulation. Given that hHcy has been reported to induce podocyte NLRP3 inflammasome activation and glomerular inflammation, our findings indicate that exosome secretion may serve as a pathogenic mechanism mediating the release of inflammatory cytokines produced by NLRP3 inflammasome in podocytes. Targeting TRPML1 channel may be a potential therapeutic strategy to attenuate podocyte-derived inflammatory exosome release and consequent glomerular inflammation during hHcy.

Declaration of competing interest

None of the authors have conflict of interest.

Acknowledgments

References

[1] C. Zhang, K.M. Boini, M. Xia, J.M. Abais, X. Li, Q. Liu, P.L. Li, Activation of Nod-like receptor protein 3 inflammasomes turns on podocyte injury and glomerular sclerosis in hyperhomocysteinemia, Hypertension 60 (2012) 154–162.

[2] J.M. Abais, M. Xia, G. Li, Y. Chen, S.M. Conley, T.W. Gehr, K.M. Boini, P.L. Li, Nod-like receptor protein 3 (NLRP3) inflammasome activation and podocyte injury via

thioredoxin-interacting protein (TXNIP) during hyperhomocysteinemia, J. Biol. Chem. 289 (2014) 27159–27168.

[3] G. Li, M. Xia, J.M. Abais, K. Boini, P.L. Li, J.K. Ritter, Protective action of anandamide and its COX-2 metabolite against l-homocysteine-induced NLRP3 inflammasome activation and injury in podocytes, J. Pharmacol. Exp. Therapeut. 358 (2016) 61–70.

[4] G. Li, Z. Chen, O.M. Bhat, Q. Zhang, J.M. Abais-Battad, S.M. Conley, J.K. Ritter, P. L. Li, NLRP3 inflammasome as a novel target for docosahexaenoic acid metabolites to abrogate glomerular injury, J. Lipid Res. 58 (2017) 1080–1090.

[5] M. Colombo, G. Raposo, C. Thery, Biogenesis, secretion, and intercellular interactions of exosomes and other extracellular vesicles, Annu. Rev. Cell Dev. Biol. 30 (2014) 255–289.

[6] J.S. Schorey, C.V. Harding, Extracellular vesicles and infectious diseases: new complexity to an old story, J. Clin. Invest. 126 (2016) 1181–1189.

[7] E. Eitan, C. Suire, S. Zhang, M.P. Mattson, Impact of lysosome status on extracellular vesicle content and release, Ageing Res. Rev. 32 (2016) 65–74.

[8] B.W. van Balkom, T. Pisitkun, M.C. Verhaar, M.A. Knepper, Exosomes and the kidney: prospects for diagnosis and therapy of renal diseases, Kidney Int. 80 (2011) 1138–1145.

[9] A. Rubartelli, F. Cozzolino, M. Talio, R. Sitia, A novel secretory pathway for interleukin-1 beta, a protein lacking a signal sequence, EMBO J. 9 (1990) 1503–1510.

[10] C.M. Boulanger, X. Loyer, P.E. Rautou, N. Amabile, Extracellular vesicles in coronary artery disease, Nat. Rev. Cardiol. 14 (2017) 259–272.

[11] D.A. Chistiakov, A.N. Orekhov, Y.V. Bobryshev, Extracellular vesicles and atherosclerotic disease, Cell. Mol. Life Sci. : CM 72 (2015) 2697–2708.

[12] N.P. Hessvik, A. Llorente, Current knowledge on exosome biogenesis and release, Cell. Mol. Life Sci. 75 (2018) 193–208.

[13] F. Baixauli, C. Lopez-Otin, M. Mittelbrunn, Exosomes and autophagy: coordinated mechanisms for the maintenance of cellular fitness, Front. Immunol. 5 (2014) 403.

[14] C.M. Fader, D. Sanchez, M. Furlan, M.I. Colombo, Induction of autophagy promotes fusion of multivesicular bodies with autophagic vacuoles in k562 cells, Traffic 9 (2008) 230–250.

[15] L. Murrow, J. Debnath, ATG12-ATG3 connects basal autophagy and late endosome function, Autophagy 11 (2015) 961–962.

[16] U. Erdbrugger, T.H. Le, Extracellular vesicles in renal diseases: more than novel biomarkers? J. Am. Soc. Nephrol. : JASN (J. Am. Soc. Nephrol.) 27 (2016) 12–26.

[17] M. Hara, T. Yanagihara, I. Kihara, K. Higashi, K. Fujimoto, T. Kajita, Apical cell membranes are shed into urine from injured podocytes: a novel phenomenon of podocyte injury, J. Am. Soc. Nephrol. : JASN (J. Am. Soc. Nephrol.) 16 (2005) 408–416.

[18] H. Lee, K.H. Han, S.E. Lee, S.H. Kim, H.G. Kang, H.I. Cheong, Urinary exosomal WT1 in childhood nephrotic syndrome, Pediatr. Nephrol. 27 (2012) 317–320.

[19] Y. Lytvyn, F. Xiao, C.R. Kennedy, B.A. Perkins, H.N. Reich, J.W. Scholey, D. Z. Cherney, D. Burger, Assessment of urinary microparticles in normotensive patients with type 1 diabetes, Diabetologia 60 (2017) 581–584.

[20] A.L. Stahl, K. Johansson, M. Mossberg, R. Kahn, D. Karpman, Exosomes and microvesicles in normal physiology, pathophysiology, and renal diseases, Pediatr. Nephrol. 34 (2019) 11–30.

[21] M. Tkaczyk, Z. Baj, Surface markers of platelet function in idiopathic nephrotic syndrome in children, Pediatr. Nephrol. 17 (2002) 673–677.

[22] J.M. Abais, M. Xia, G. Li, T.W. Gehr, K.M. Boini, P.L. Li, Contribution of endogenously produced reactive oxygen species to the activation of podocyte NLRP3 inflammasomes in hyperhomocysteinemia, Free Radical Biol. Med. 67 (2014) 211–220.

[23] J.M. Abais, C. Zhang, M. Xia, Q. Liu, T.W. Gehr, K.M. Boini, P.L. Li, NADPH oxidase-mediated triggering of inflammasome activation in mouse podocytes and glomeruli during hyperhomocysteinemia, Antioxidants Redox Signal. 18 (2013) 1537–1548.

[24] Y. Yuan, Y. Chen, T. Peng, L. Li, W. Zhu, F. Liu, S. Liu, X. An, R. Luo, J. Cheng, J. Liu, Y. Lu, Mitochondrial ROS-induced lysosomal dysfunction impairs autophagic flux and contributes to M1 macrophage polarization in a diabetic condition, Clin. Sci. 133 (2019) 1759–1777.

[25] S.B. Song, E.S. Hwang, High levels of ROS impair lysosomal acidity and autophagy flux in glucose-deprived fibroblasts by activating ATM and erk pathways, Biomolecules 10 (2020).

[26] G. Li, D. Huang, J. Hong, O.M. Bhat, X. Yuan, P.L. Li, Control of lysosomal TRPML1 channel activity and exosome release by acid ceramidase in mouse podocytes, Am. J. Physiol. Cell Physiol. 317 (2019) C481–C491.

[27] G. Li, D. Huang, O.M. Bhat, J.L. Poklis, A. Zhang, Y. Zou, J. Kidd, T.W.B. Gehr, P. L. Li, Abnormal podocyte TRPML1 channel activity and exosome release in mice with podocyte-specific Asah1 gene deletion, Biochim. Biophys. Acta Mol. Cell Biol. Lipids 1866 (2020), 158856.

[28] W. Maciel, W.D. Lopes, B. Cruz, W. Teixeira, G. Felippelli, C.A. Sakamoto, F. C. Favero, C. Buzzulini, V. Soares, L.V. Gomes, M. Bichuette, A.J. da Costa, Effects of Haematobia irritans infestation on weight gain of Nelore calves assessed with different antiparasitic treatment schemes, Prev. Vet. Med. 118 (2015) 182–186.

[29] F. Martinon, A. Mayor, J. Tschopp, The inflammasomes: guardians of the body, Annu. Rev. Immunol. 27 (2009) 229–265.

[30] C.M. Cruz, A. Rinna, H.J. Forman, A.L. Ventura, P.M. Persechini, D.M. Ojcius, ATP activates a reactive oxygen species-dependent oxidative stress response and secretion of proinflammatory cytokines in macrophages, J. Biol. Chem. 282 (2007) 2871–2879.

[31] A. Halle, V. Hornung, G.C. Petzold, C.R. Stewart, B.G. Monks, T. Reinheckel, K. A. Fitzgerald, E. Latz, K.J. Moore, D.T. Golenbock, The NALP3 inflammasome is involved in the innate immune response to amyloid-beta, Nat. Immunol. 9 (2008) 857–865.

[32] A.M. Nour, Y.G. Yeung, L. Santambrogio, E.D. Boyden, E.R. Stanley, J. Brojatsch, Anthrax lethal toxin triggers the formation of a membrane-associated inflammasome complex in murine macrophages, Infect. Immun. 77 (2009) 1262–1271.

[33] G. Li, J. Kidd, P.L. Li, Podocyte lysosome dysfunction in chronic glomerular diseases, Int. J. Mol. Sci. 21 (2020).

[34] M. Hara, K. Yamagata, Y. Tomino, A. Saito, Y. Hirayama, S. Ogasawara, H. Kurosawa, S. Sekine, K. Yan, Urinary podocalyxin is an early marker for podocyte injury in patients with diabetes: establishment of a highly sensitive ELISA to detect urinary podocalyxin, Diabetologia 55 (2012) 2913–2919.

[35] X. Wu, Y. Gao, L. Xu, W. Dang, H. Yan, D. Zou, Z. Zhu, L. Luo, N. Tian, X. Wang, Y. Tong, Z. Han, Exosomes from high glucose-treated glomerular endothelial cells trigger the epithelial-mesenchymal transition and dysfunction of podocytes, Sci. Rep. 7 (2017) 9371.

[36] H. Castrop, I.M. Schiessl, Novel routes of albumin passage across the glomerular filtration barrier, Acta Physiol. 219 (2017) 544–553.

[37] J. Hong, O.M. Bhat, G. Li, S.K. Dempsey, Q. Zhang, J.K. Ritter, W. Li, P.L. Li, Lysosomal regulation of extracellular vesicle excretion during d-ribose-induced NLRP3 inflammasome activation in podocytes, Biochimica et biophysica acta, Molecular cell research 1866 (2019) 849–860.

[38] J. Xiong, M. Xia, M. Xu, Y. Zhang, J.M. Abais, G. Li, C.R. Riebling, J.K. Ritter, K. M. Boini, P.L. Li, Autophagy maturation associated with CD38-mediated regulation of lysosome function in mouse glomerular podocytes, J. Cell Mol. Med. 17 (2013) 1598–1607.

[39] J.X. Bao, Q.F. Zhang, M. Wang, M. Xia, K.M. Boini, E. Gulbins, Y. Zhang, P.L. Li, Implication of CD38 gene in autophagic degradation of collagen I in mouse coronary arterial myocytes, Front. Biosci. 22 (2017) 558–569.

[40] M. Xu, X. Li, S.W. Walsh, Y. Zhang, J.M. Abais, K.M. Boini, P.L. Li, Intracellular two-phase Ca2+ release and apoptosis controlled by TRP-ML1 channel activity in coronary arterial myocytes, American journal of physiology, Cell physiology 304 (2013) C458–C466.

[41] F. Zhang, M. Xu, W.Q. Han, P.L. Li, Reconstitution of lysosomal NAADP-TRP-ML1 signaling pathway and its function in TRP-ML1(-/-) cells, American journal of physiology, Cell physiology 301 (2011) C421–C430.

[42] D. Shen, X. Wang, X. Li, X. Zhang, Z. Yao, S. Dibble, X.P. Dong, T. Yu, A. P. Lieberman, H.D. Showalter, H. Xu, Lipid storage disorders block lysosomal trafficking by inhibiting a TRP channel and lysosomal calcium release, Nat. Commun. 3 (2012) 731.

[43] M. Sun, E. Goldin, S. Stahl, J.L. Falardeau, J.C. Kennedy, J.S. Acierno Jr., C. Bove, C.R. Kaneski, J. Nagle, M.C. Bromley, M. Colman, R. Schiffmann, S. A. Slaugenhaupt, Mucolipidosis type IV is caused by mutations in a gene encoding a novel transient receptor potential channel, Hum. Mol. Genet. 9 (2000) 2471–2478.

[44] G.C. Churchill, Y. Okada, J.M. Thomas, A.A. Genazzani, S. Patel, A. Galione, NAADP mobilizes Ca(2+) from reserve granules, lysosome-related organelles, in sea urchin eggs, Cell 111 (2002) 703–708.

[45] A. Galione, NAADP, a new intracellular messenger that mobilizes Ca2+ from acidic stores, Biochem. Soc. Trans. 34 (2006) 922–926.

[46] F. Zhang, M. Xia, P.L. Li, Lysosome-dependent Ca(2+) release response to Fas activation in coronary arterial myocytes through NAADP: evidence from CD38 gene knockouts, American journal of physiology, Cell physiology 298 (2010) C1209–C1216.

[47] F. Zhang, G. Zhang, A.Y. Zhang, M.J. Koeberl, E. Wallander, P.L. Li, Production of NAADP and its role in Ca2+ mobilization associated with lysosomes in coronary arterial myocytes, American journal of physiology, Heart and circulatory physiology 291 (2006) H274–H\282.

[48] X.P. Dong, D. Shen, X. Wang, T. Dawson, X. Li, Q. Zhang, X. Cheng, Y. Zhang, L. S. Weisman, M. Delling, H. Xu, PI(3,5)P(2) controls membrane trafficking by direct activation of mucolipin Ca(2+) release channels in the endolysosome, Nat. Commun. 1 (2010) 38.

[49] X.P. Dong, X. Cheng, E. Mills, M. Delling, F. Wang, T. Kurz, H. Xu, The type IV mucolipidosis-associated protein TRPML1 is an endolysosomal iron release channel, Nature 455 (2008) 992–996.

[50] X. Li, N. Rydzewski, A. Hider, X. Zhang, J. Yang, W. Wang, Q. Gao, X. Cheng, H. Xu, A molecular mechanism to regulate lysosome motility for lysosome positioning and tubulation, Nat. Cell Biol. 18 (2016) 404–417.

[51] X. Zhang, X. Cheng, L. Yu, J. Yang, R. Calvo, S. Patnaik, X. Hu, Q. Gao, M. Yang, M. Lawas, M. Delling, J. Marugan, M. Ferrer, H. Xu, MCOLN1 is a ROS sensor in lysosomes that regulates autophagy, Nat. Commun. 7 (2016) 12109.

[52] M.B. Morelli, C. Amantini, D. Tomassoni, M. Nabissi, A. Arcella, G. Santoni, Transient receptor potential mucolipin-1 channels in glioblastoma: role in patient's survival, Cancers (2019) 11.

[53] J. Cui, L. Tang, Q. Hong, S. Lin, X. Sun, G. Cai, X.Y. Bai, X. Chen, N-acetylcysteine ameliorates gentamicin-induced nephrotoxicity by enhancing autophagy and reducing oxidative damage in miniature pigs, Shock 52 (2019) 622–630.

[54] S. Chowdhury, S. Ghosh, A.K. Das, P.C. Sil, Ferulic acid protects hyperglycemia-induced kidney damage by regulating oxidative insult, inflammation and autophagy, Front. Pharmacol. 10 (2019) 27.

[55] X.Y. Wang, H. Yang, M.G. Wang, D.B. Yang, Z.Y. Wang, L. Wang, Trehalose protects against cadmium-induced cytotoxicity in primary rat proximal tubular cells via inhibiting apoptosis and restoring autophagic flux, Cell Death Dis. 8 (2017), e3099.

[56] J.M. Abais, M. Xia, Y. Zhang, K.M. Boini, P.L. Li, Redox regulation of NLRP3 inflammasomes: ROS as trigger or effector? Antioxidants Redox Signal. 22 (2015) 1111–1129.

[57] H. Cai, K.K. Griendling, D.G. Harrison, The vascular NAD(P)H oxidases as therapeutic targets in cardiovascular diseases, Trends Pharmacol. Sci. 24 (2003) 471–478.

[58] M. Xia, K.M. Boini, J.M. Abais, M. Xu, Y. Zhang, P.L. Li, Endothelial NLRP3 inflammasome activation and enhanced neointima formation in mice by adipokine visfatin, Am. J. Pathol. 184 (2014) 1617–1628.

[59] M. Xia, C. Zhang, K.M. Boini, A.M. Thacker, P.L. Li, Membrane raft-lysosome redox signalling platforms in coronary endothelial dysfunction induced by adipokine visfatin, Cardiovasc. Res. 89 (2011) 401–409.

[60] J.Y. Youn, K.L. Siu, H.E. Lob, H. Itani, D.G. Harrison, H. Cai, Role of vascular oxidative stress in obesity and metabolic syndrome, Diabetes 63 (2014) 2344–2355.

[61] J. Jiang, K. Huang, S. Xu, J.G.N. Garcia, C. Wang, H. Cai, Targeting NOX4 alleviates sepsis-induced acute lung injury via attenuation of redox-sensitive activation of CaMKII/ERK1/2/MLCK and endothelial cell barrier dysfunction, Redox biology 36 (2020), 101638.